CHARACTERISATION OF NANOCOMPOSITE THERMOSENSITIVE HYDROGELS BASED ON CHITOSAN AND CARBON NANOTUBES

Katarzyna Pieklarz[1,a,*], Zofia Modrzejewska[1,b], Grzegorz Galita[2,c], Ireneusz Majsterek[2,d]

[1] – Department of Environmental Engineering, Faculty of Process and Environmental Engineering, Lodz University of Technology, Wólczańska 215 Str., 93-005 Łódź, Poland

[a] – ORCID: 0009-0009-8398-9398, [b] – ORCID: 0000-0001-6133-7684

[2] – Department of Clinical Chemistry and Biochemistry, Medical University of Lodz, Mazowiecka 5 Str., 92-215 Łódź, Poland

[c] – ORCID: 0000-0002-1559-2796, [d] – ORCID: 0000-0001-6231-3334

**corresponding author: katarzyna.pieklarz@p.lodz.pl*

Abstract

In recent years, the polymer nanocomposites containing carbon nanotubes have been the subject of intense research. Chitosan-based systems are particularly promising due to the unique biological properties of this polysaccharide. This article presents the results of research on thermosensitive chitosan hydrogels containing single-walled carbon nanotubes. Biomaterials were prepared from chitosan lactate and chitosan chloride solutions using β-glycerol phosphate disodium salt pentahydrate as the cross-linking agent. A preliminary characterisation of the developed systems was performed. The nanocomposite hydrogels were analysed using Fourier transform infrared spectroscopy (FTIR) and differential scanning calorimetry (DSC). Additionally, the cytotoxicity of the biomaterials against normal human BJ fibroblasts was assessed using the resazurin assay. The studies suggest that chitosan hydrogels containing carbon nanotubes may be promising solutions for biomedical applications.

Keywords: *chitosan, biomaterials, thermosensitive hydrogel, carbon nanotubes, biomedical applications*

Received: 19.04.2026
Accepted: 24.07.2026

1. Introduction

The current intensive progress in the fields of reconstructive and regenerative medicine, as well as tissue engineering, is primarily due to the availability of innovative materials developed to meet medical requirements. In clinical practice, various materials, such as metals, polymers, and ceramics, are used to reconstruct or regenerate damaged tissues [1].

Among the polymers that have gained significant recognition in the biomedical field, chitosan occupies a special position. Structurally, it is an unbranched copolymer of β-(1→4)-2-acetamido-D-glucose (*N*-acetyl-D-glucosamine, GlcNAc) and β-(1→4)-2-amino-D-glucose (D-glucosamine, GlcN). It should be emphasised that the GlcNAc and GlcN residues are randomly distributed and not blocked together [2, 3]. The interest in chitosan is mainly due to its unique biological properties. This polymer is characterised by non-toxicity, biocompatibility with living tissues, and biodegradability. It exhibits antibacterial, antifungal, anti-inflammatory, non-allergenic, antioxidant, and anticancer properties [4–6]. Chitosan's ability to form a wide variety of morphological structures, such as fibres and nanofibres, gels, sponges, films, membranes, and scaffolds [7, 8], is also advantageous.

Nevertheless, new solutions are continually sought to improve polymer properties, thereby expanding the range of their medical applications. The greatest interest concerns the use of nanocomposite materials [9]. Nanofillers introduced into the biocompatible polymer matrices influence their properties, which is important for both structural implants and materials intended for tissue regeneration. Nanoparticles can influence the material surface topography and effectively modify mechanical parameters such as stiffness and strength [9]. Combinations of chitosan with nanostructured carbon materials, such as carbon nanotubes, which are cylindrically rolled graphene layers connected by the edges, in which the carbon atoms are of the sp^2 configuration [10], are particularly promising.

Chitosan-carbon nanotube systems can be used, among other applications, as wound-dressing materials with high antibacterial activity against Gram-negative and Gram-positive bacteria [11–13] or as drug carriers, primarily for chemotherapeutics [14–16]. Additionally, these nanocomposites show significant potential for use in gene therapy [17–19], tissue engineering [20–23], and the construction of biosensors characterised by high sensitivity and selectivity [24, 25].

However, it should be emphasised that the biocompatibility and potential toxicity of nanostructured carbon materials remain unresolved [26, 27]. Many factors determine the biocompatibility of carbon nanotubes, often not directly related to the nanotubes themselves. An example is the presence of metal catalysts used in their synthesis. Transition-metal residues, primarily iron, in nanotubes can generate reactive oxygen species (ROS) via the Fenton reaction. An imbalance between ROS (free radicals) activity and the biological capacity to rapidly detoxify reactive intermediates can contribute to oxidative stress and, consequently, cell death [28]. Furthermore, the tendency of nanotubes to agglomerate is an important issue, which significantly affects cellular and tissue responses. In the case of nanotubes that form agglomerates, phagocytosis is hindered, leading to the production of proinflammatory and toxic substances and, ultimately, cell death [28].

In this research, the nanocomposite thermosensitive chitosan hydrogels containing carbon nanotubes are characterised. Biomaterials were fabricated from solutions of two chitosan salt types: chitosan lactate and chitosan chloride. β-glycerol phosphate disodium salt pentahydrate (β-GP) was used as a cross-linking agent.

Thermosensitive hydrogels are a class of smart hydrogels that change from a sol to a gel state upon temperature change. A key parameter of these systems is the critical solution temperature (CST), at which the polymer-solvent (water) system undergoes a phase transition. The lower critical solution temperature (LCST) is the minimum temperature needed for the sol-gel transition of thermally responsive polymers. On the other hand, the upper critical solution temperature (UCST) indicates that the gel structure forms below this temperature, and the polymer dissolves when heated above it [29–31]. The main advantage of thermosensitive hydrogels is their ability to form *in situ*. When applied to living organisms, these biomaterials can fill damaged sites, even those of complex shapes. Furthermore, these hydrogels gradually degrade *in vivo*, eliminating the need for a reoperation and providing greater patient comfort [31].

The presented studies involved both structural characterisation and thermal analysis of the developed hydrogels. Furthermore, the *in vitro* biological experiments assessed the potential cytotoxicity of the biomaterials towards normal human BJ fibroblasts.

The aim of the research was to verify whether the introduction of carbon nanotubes into the polymer matrix would affect the structural, thermal, and biocompatibility properties of the developed systems compared with unmodified hydrogels.

2. Materials and Methods

2.1. Materials

The following chemical reagents were used to prepare the nanocomposite hydrogels: chitosan (CH) (product no. 50494, CAS no. 9012-76-4, weight average molecular mass M_w = 680 kg/mol, number average molecular mass M_n = 110 kg/mol, degree of acetylation DA = 18.2%); lactic acid (LA) (product no. L6661, CAS no. 50-21-5); hydrochloric acid (HCl) (product no. H1758, CAS no. 7647-01-0); single-walled carbon nanotubes (CNTs) (product no. 724777, CAS no. 308068-56-6, average diameter: 1.3 nm, median length: 1 μm); β-glycerol phosphate disodium salt pentahydrate (β-GP) (product no. 50020, CAS no. 13408-09-8). All reagents were procured from Sigma-Aldrich (Poznan, Poland).

2.2. Methods

2.2.1. Preparation of the Aqueous Dispersion of Carbon Nanotubes

The aqueous CNT dispersion at 0.1% (w/v) was prepared by sonication of the CNT powder in ultrapure deionised water. The sodium dodecyl sulfate (SDS) (Sigma-Aldrich, Poznan, Poland, product no. L5750, CAS no. 151-21-3) surfactant was applied to stabilise the CNTs dispersion. Precisely, the CNTs powder was mixed with an aqueous SDS solution at 1.5% (w/w), and the resulting mixture was sonicated for c.a. 1 h in an ultrasonic bath at 24°C [32–34].

2.2.2. Preparation of the Nanocomposite Hydrogels

The thermosensitive nanocomposite chitosan hydrogels were prepared by physical blending of the components. Firstly, the chitosan salt solution (2.5% (w/v)) was prepared by dissolving 0.4 g of CH in 16 mL of 0.1 mol/L LA or HCl, and then left at room temperature for 24 h. In the next step, a 0.1% (w/v) water dispersion of CNTs was added dropwise to the chitosan solution. The sample was mixed for 30 min. The mass concentrations of CNTs in the chitosan salt solutions were 0.028, 0.055, and 0.1 $mg_{CNTs}/mL_{chit.salt}$. The samples were stored in a laboratory refrigerator for 2 h to reach ca. 4 °C.

https://doi.org/10.15259/PCACD.31.009

Simultaneously, a cross-linking agent suspension was prepared (2 g of β-GP dissolved in 2 mL of deionised water at 4 °C) and added dropwise to the chitosan salt solution containing CNTs; then mixed for ca. 10 min. The prepared formulations were left in a refrigerator for 2 h to remove air bubbles that formed during mixing. Then, the biomaterials were stored at 37 °C to allow gelation to complete.

Unmodified chitosan systems, without CNTs, were fabricated as a control group. The final products were frozen at −20 °C and then lyophilised [35, 36].

2.2.3. Physicochemical Analysis

The structure of the lyophilised chitosan hydrogels was determined using Fourier Transform Infrared Spectroscopy (FTIR). The spectra were obtained using the Nicolet™ iS50 FT-IR apparatus equipped with a monolithic diamond ATR crystal (Thermo Fisher Scientific Inc., Waltham, MA, USA). FTIR spectra were recorded with 100 scans at a 4.0 cm^{-1} resolution in the wavenumber range of 500–4000 cm^{-1}.

Thermal studies of the obtained materials were performed using Differential Scanning Calorimetry (DSC, FP 90, Mettler-Toledo). The lyophilised hydrogels (~10 mg) were examined in aluminium crucibles over a 30–200°C temperature range at a heating rate of 10 °C/min. DSC thermograms were analysed using thermal analysis software (FP99).

2.2.4. Biological Characterisation

The cytotoxicity of the developed hydrogels was assessed against a normal human fibroblast cell line BJ (ATCC® CRL-2522™), purchased from the American Type Culture Collection (ATCC, Manassas, VA, USA).

The cells were cultured under standard conditions (5% CO_2, 95% humidity, 37 °C) in Eagle's Minimum Essential Medium (EMEM) (Sigma-Aldrich Corp., St. Louis, MO, USA) supplemented with 2 mM L-glutamine (GIBCO-BRL, Life Technologies Ltd., Paisley, UK), 10% (v/v) fetal bovine serum (FBS) (Sigma-Aldrich Corp., St. Louis, MO, USA), 100 units/mL penicillin and 100 µg/mL streptomycin (GIBCO-BRL, Life Technologies Ltd., Paisley, UK). After exposure to accutase solution, the cells were passaged at 70–80% confluency.

To evaluate the cytotoxicity of the hydrogels on the studied cell line, the colourimetric resazurin assay (In Vitro Toxicology Assay Kit, Resazurin-based, Sigma-Aldrich Corp., St. Louis, MO, USA) was performed. All analyses were carried out in triplicate. BJ cells were seeded in 12-well plates ($2 \cdot 10^5$ cells/well) and cultured in 1 mL of complete Eagle's Minimum Essential Medium for 24 h. The cells suspended in the complete culture medium served as a negative control, whereas cells treated with 100% DMSO (Sigma-Aldrich Corp., St. Louis, MO, USA) served as a positive control. After cell adhesion, the cells were incubated with hydrogels (5 mm in diameter) for 48 h. Following incubation, the well contents were removed, and the cells were rinsed twice with 1 X DPBS (Sigma-Aldrich Corp., St. Louis, MO, USA). Subsequently, 100 µL of the resazurin solution was added to each well, and the cells were incubated for 2 h. Absorbance was measured at 600 nm and 690 nm (reference) using the Synergy HT spectrophotometer (BioTek, Hong Kong, China).

The statistical analysis was performed in the Statistica 13 program (StatSoft, Kraków, Poland). Statistical significance was assessed using the one-way analysis of variance (ANOVA) and Dunnett's multiple comparison post hoc test. Research results were expressed as mean ± standard deviation (SD) from three independent experiments. In the graphs, the differences were statistically significant as follows: $*p < 0.05$, $**p < 0.01$, and $***p < 0.001$ relative to the negative control.

3. Results and Discussion

3.1. Structural Characteristics of the Nanocomposite Chitosan Hydrogels

Figures 1 and 2 present the FTIR spectra of chitosan lactate-based nanocomposite hydrogels with β-GP and, as a reference, the spectrum of the unmodified system (CH/LA/β-GP).

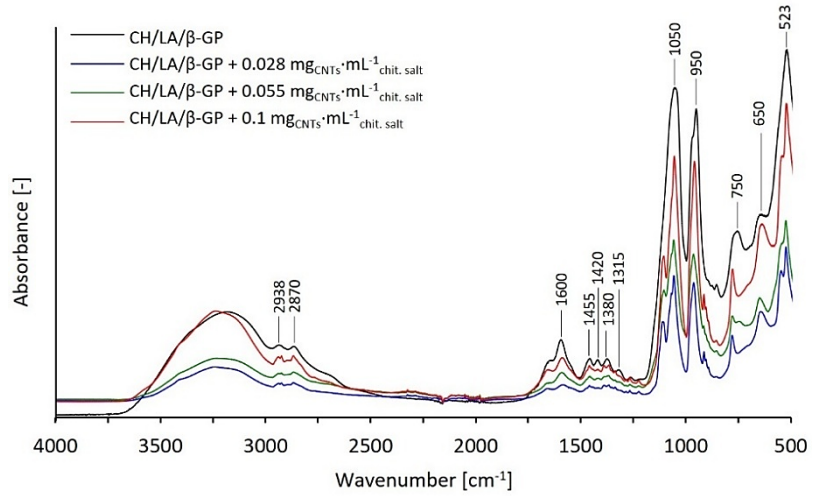

Figure 1. Full-range FTIR spectra of CH/LA/β-GP with different concentrations of CNTs.

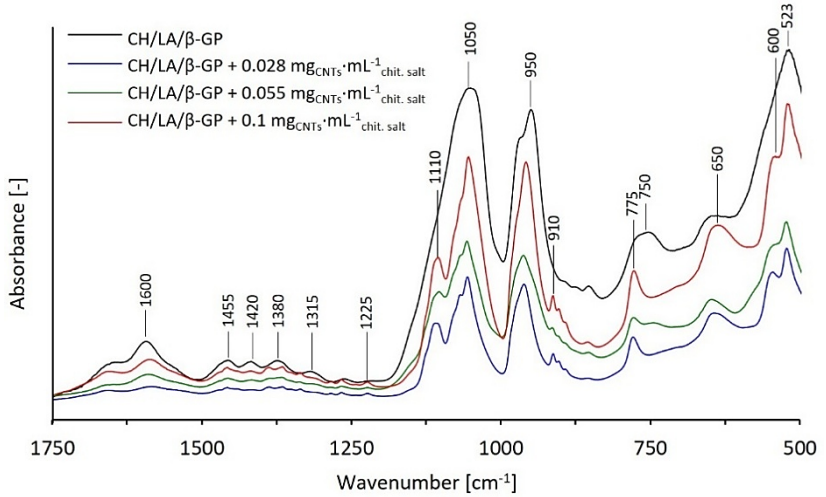

Figure 2. FTIR spectra of CH/LA/β-GP with different concentrations of CNTs (500–1750 cm^{-1}).

It can be observed that the introduction of CNTs at 0.028, 0.055 and 0.1 mg$_{CNTs}$/mL$_{chit.salt}$ mass concentrations to the chitosan lactate solutions caused changes in the intensity of the absorption bands, also observed in the spectrum of the control sample (CH/LA/β-GP), described in detail by us earlier [37]. With increasing carbon nanotube concentration, band intensities across the entire wavenumber range increase; however, the intensity of

the bands in the sample with the highest CNT concentration never exceeds that of the absorption bands observed for the control.

The above-identified trends concern: (i) a broad, asymmetric band occurring in the 3000–3600 cm^{-1} range (the band representing the stretching vibrations of the –OH group and the overlapping stretching vibrations of the N–H bonds in the amino and acetamide groups), (ii) signals in the 2850–2950 cm^{-1} region (related to the symmetric and asymmetric stretching vibrations of the –CH groups from the chitosan pyranose ring and the stretching vibrations of the C-H bonds in the $–CH_2–$ and $–CH_3$ groups assigned to the ring), (iii) the range comprising amide bands, and (iv) the 1200–1500 cm^{-1} region. Additionally, for the modified hydrogels, a peak at 1225 cm^{-1}, associated with C-O stretching vibrations and corresponding to internal defects in carbon nanotubes [38], is observed.

The most pronounced differences in the spectra of the modified systems are observed in the range of 800–1200 cm^{-1}; the region characteristic of the saccharide structure. As the nanofiller concentration increases, the intensity of two main bands at 1050 cm^{-1}, corresponding to the asymmetric P-O-C stretching vibrations, and at 950 cm^{-1}, which may indicate the presence of the diprotonated phosphate group ($H_2PO_4^-$), increases, but these peaks are still lower in intensity than the corresponding bands observed for the control sample. However, a shoulder at 1110 cm^{-1} and a signal at 910 cm^{-1} become clearly visible. The increase in the intensity of the above signals may result from non-covalent interactions (mainly hydrogen bonds and CH-π interactions) between the polymer matrix and the surface of carbon nanotubes, which consequently lead to local ordering and stiffening of chitosan chains [39]. Furthermore, the band at 750 cm^{-1} (characteristic of β-GP and corresponding to the symmetric P-O-C stretching vibrations) observed for the control shifts to 775 cm^{-1} in the modified samples, while the signal at 523 cm^{-1} shows a shoulder at 600 cm^{-1}.

Figures 3 and 4 illustrate the FTIR spectra of the nanocomposite hydrogels based on the chitosan chloride solutions with β-GP, and additionally, as a reference point, the spectrum of the sample without the nanofiller (CH/HCl/β-GP).

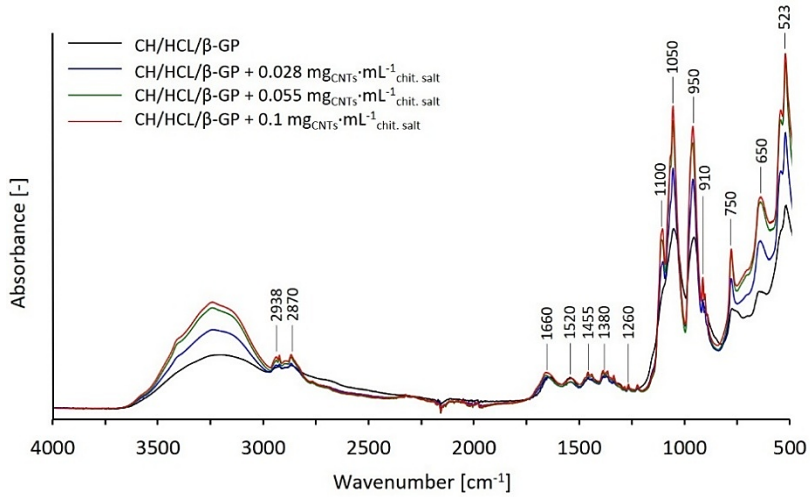

Figure 3. Full-range FTIR spectra of CH/HCl/β-GP with different concentrations of CNTs.

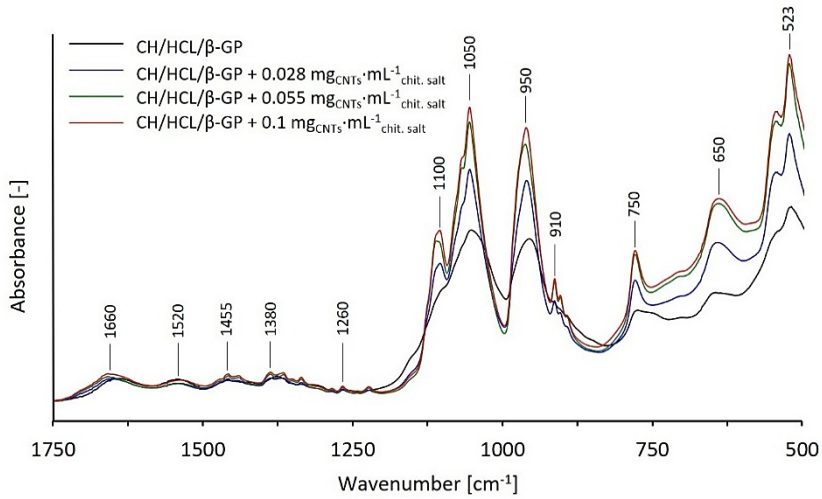

Figure 4. FTIR spectra of CH/HCl/β-GP with different concentrations of CNTs (500–1750 cm^{-1}).

Considering the characteristics of the recorded spectra, it can be concluded that the introduction of CNTs into the chitosan chloride with β-GP, similar to the previously discussed hydrogel variants, contributed to changes in the intensity of the bands identified for the control (CH/HCl/β-GP) [37]. Over the entire wavenumber range (500–4000 cm^{-1}), it can be observed that with increasing concentration of carbon nanotubes, the intensity of absorption bands increases, and the intensity is always higher than that of the unmodified sample.

The principal differences in the spectra of the systems with the nanofiller are observed only in the range of 800–1200 cm^{-1}. As the CNT concentration increases, the intensity of the two main bands at 1050 and 950 cm^{-1} increases. Additionally, a shoulder at 1100 cm^{-1} and a signal at 910 cm^{-1} become visible.

Analysing the FTIR spectra of hydrogels prepared from chitosan lactate and chitosan chloride solutions, it can be observed that the introduction of carbon nanotubes into the polymer matrix did not result in any new absorption bands characteristic of the nanofiller used, nor did it cause any significant shifts in bands relative to the control. This suggests that the overall chemical structure of the polymer was not altered, which in turn may indicate that the interactions between the chitosan matrix and carbon nanotubes are primarily non-covalent ones [39].

3.2. Thermal Analysis of the Chitosan Systems

The thermal properties of the lyophilised chitosan hydrogels were characterised using differential scanning calorimetry (DSC), which enables the determination of the thermal effects of endothermic and exothermic processes.

Polysaccharides, including chitosan, belong to the group of hydrophilic polymers whose hydration properties are determined by their molecular and supramolecular structures [40]. Depending on the type of interactions between water molecules and polymer chains, water release from the polysaccharide matrix occurs at various temperatures. In DSC thermograms, the endothermic peaks correspond to the loss of water bound to the polymers' hydrophilic groups, while the exothermic peaks indicate chitosan degradation resulting from dehydration and depolymerisation. It should be emphasised

that thermal degradation of chitosan begins at ~250°C [41, 42], which allowed us to set the final temperature of DSC measurements at 200°C.

Figures 5 and 6, as well as Table 1, show the DSC results obtained for the developed nanocomposite biomaterials.

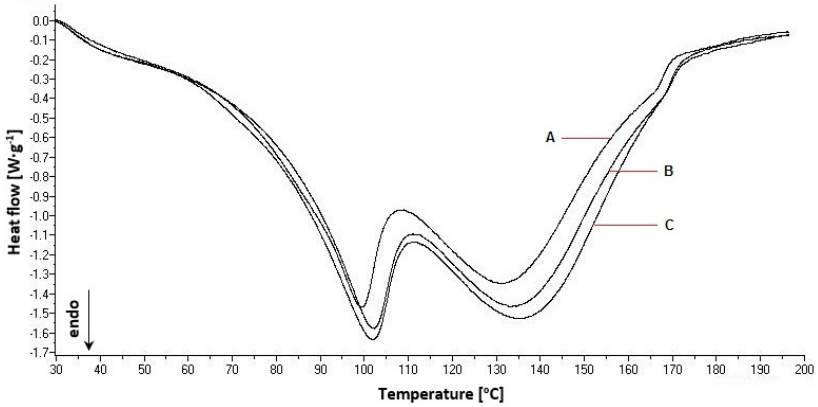

Figure 5. DSC curves of (a) CH/LA/β-GP, (b) CH/LA/β-GP + 0.028 $mg_{CNTs}/mL_{chi.salt}$, and (c) CH/LA/β-GP + 0.1 $mg_{CNTs} \cdot mL^{-1}_{chi.salt}$.

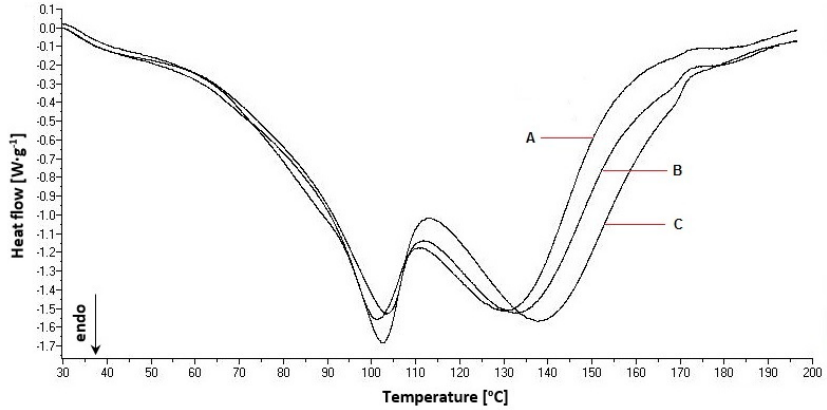

Figure 6. DSC curves of (a) CH/HCl/β-GP system, (b) CH/HCl/β-GP + 0.028 $mg_{CNTs}/mL_{chi.salt}$, and (c) CH/HCl/β-GP + 0.1 $mg_{CNTs} \cdot mL_{chi.salt}$.

Based on the analyses conducted, a broad, double-peaked endothermic band is observed in the DSC thermal curves for all systems prepared using chitosan lactate solutions (Figure 5). The appearance of this peak is most likely due to the gradual evaporation of water from the pores of the hydrogels, despite the long, careful drying process of the samples. This double peak may indicate a heterogeneous pore structure in the analysed samples. In porous materials, water evaporation is limited by the pore network, which can delay the complete removal of moisture from the sample [43]. Peaks observed at lower temperatures likely represent the evaporation of water present in larger pores, while peaks at higher temperatures may indicate the evaporation of water present in smaller, more confined pores. Water entrapment in smaller pores increases the enthalpy of water vaporisation and the temperature required for its release.

Table 1. Thermal properties of the different chitosan hydrogels.

Sample	T [°C] of water evaporation		ΔH [J/g]
CH/LA/β-GP	99.5	131.8	457.6
CH/LA/β-GP + 0.028 $mg_{CNTs}/mL_{chit.salt}$	101.8	134.1	517.8
CH/LA/β-GP + 0.1 $mg_{CNTs}/mL_{chit.salt}$	102.1	135.0	569.3
CH/HCl/β-GP	101.5	131.0	518.5
CH/HCl/β-GP + 0.028 $mg_{CNTs}/mL_{chit.salt}$	102.5	133.5	525.9
CH/HCl/β-GP + 0.1 $mg_{CNTs}/mL_{chit.salt}$	103.5	138.2	546.7

Analogous results were obtained for the hydrogels based on chitosan chloride solutions (Figure 6) – the thermograms are similar to those of the chitosan lactate samples. In this case, a broad endotherm with two peaks is also observed.

It should be emphasised that for the modified hydrogels fabricated from both types of chitosan salt solutions, a slight shift in the endothermic band maxima towards higher values is observed, compared to the results obtained for the samples without the nanofiller. Carbon nanotubes likely impose a form of geometric confinement, reducing the mobility of water molecules while increasing the energy required to release them from the material structure [44].

3.3. Evaluation of the Cytotoxicity of Chitosan Hydrogels

To assess the biological properties of materials intended for biomedical use, it is necessary to conduct thorough research in accordance with applicable standards. This applies particularly to materials intended for an implantation, for which the evaluation criteria are stringent. Biomaterials must be the best possible substitute for the recipient's tissue and, at the same time, be biocompatible. Therefore, they must be capable of fulfilling a biological function in a specific application and, above all, they must not cause cytotoxicity to the patient's cells and tissues [28].

Consequently, the cytotoxic activity of the developed chitosan systems containing the carbon nanofiller against normal human BJ fibroblasts was evaluated. The use of this cell line in biological studies resulted from the widespread occurrence of fibroblasts in the human body (the main and most numerous cells of the connective tissue) and from their high metabolic activity, including the production of extracellular matrix components (glycosaminoglycans, collagen). Studies with fibroblasts enable verification of the ability of biomaterial surfaces to integrate with connective tissue and provide information on the potential to limit fibrosis [28, 45].

The results of the cytotoxicity analysis are illustrated in Figure 7. The analysis of cytotoxic activity of the developed nanocomposite chitosan hydrogels, measured by a colourimetric assay based on the reduction of resazurin to resorufin [36], showed that after 48 h of incubation of BJ cells with the control sample (without CNT) and the CH/LA/β-GP system containing 0.028 $mg_{CNTs}/mL_{chit.salt}$ the cell viability reached 101.91 ± 6.46% and 92.24 ± 6.16%, respectively. Similar results were obtained for the CH/HCl/β-GP hydrogels containing analogous nanofiller doses: cell viability was 94.33 ± 5.58% and 90.67 ± 2.85%, respectively. The above systems did not induce cytotoxic effects in BJ cells, meeting both the provisions of ISO 10993-5:2009 [46] and the more restrictive criteria set by Dahl *et al.* [47]. No statistically significant differences between the fibroblast's viability exposed to the above biomaterials and the negative control were noted ($p > 0.05$).

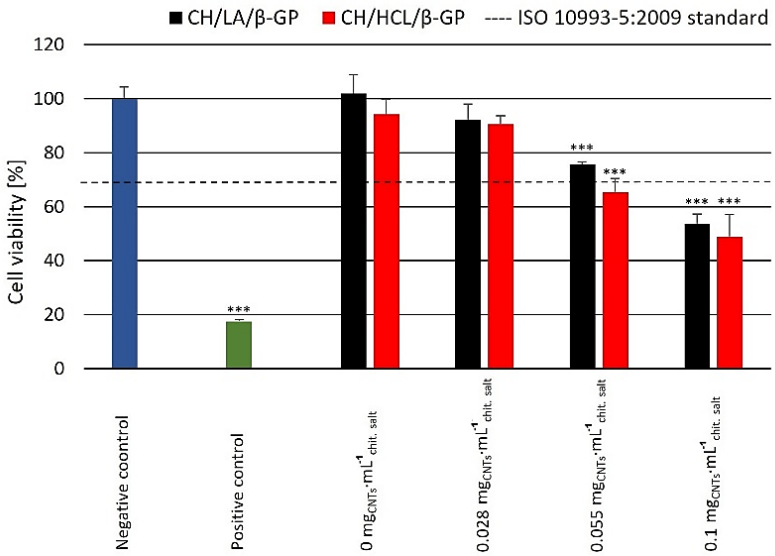

Figure 7. BJ cells' viability in the resazurin assay after exposure to the nanocomposite chitosan hydrogels (*** $p < 0.001$ versus negative control).

Hydrogels fabricated from both types of chitosan salt solutions with CNTs at 0.055 $mg_{CNTs}/mL_{chit.salt}$ demonstrated slight cytotoxicity according to the Dahl *et al.* [47] classification. For these systems, the cell viability was: 75.77 ± 0.70% (CH/LA/β-GP + 0.055 $mg_{CNTs}/mL_{chit.salt}$) and 65.38 ± 4.62% (CH/HCl/β-GP + 0.055 $mg_{CNTs}/mL_{chit.salt}$), which turned out to be statistically significant with respect to the negative control (***$p < 0.001$).

Finally, the hydrogels with the highest nanofiller concentration showed moderate cytotoxicity [47]. For these systems, the BJ cell viability was: 53.67 ± 4.75% (CH/LA/β-GP + 0.1 $mg_{CNTs}/mL_{chit.salt}$) and 48.88 ± 7.52% (CH/HCl/β-GP + 0.1 $mg_{CNTs}/mL_{chit.salt}$), which was also statistically significant with respect to the negative control (***$p < 0.001$).

4. Conclusion

Based on the conducted studies, the following conclusion can be drawn:

1. The introduction of carbon nanotubes into the chitosan lactate and chitosan chloride hydrogels with β-GP resulted only in changes in absorption intensity in the FTIR spectra of the control samples (the unmodified hydrogels). The absence of peaks typical of carbon nanotubes and the absence of major spectral shifts suggest that introducing the nanofiller into the polymer matrix likely causes only surface-level alterations in the analysed chitosan systems, without affecting the polymer's chemical structure or altering the cross-linking environment.
2. The DSC thermograms of all chitosan hydrogels show a broad, double-peaked endothermic band, which probably indicates the gradual evaporation of water contained in the pores of the hydrogels, despite the long drying of the samples.
3. Biomaterials fabricated from the chitosan lactate and chitosan chloride solutions containing a low concentration of the nanofiller (0.028 $mg_{CNTs}/mL_{chit.salt}$) did not induce cytotoxicity towards BJ fibroblasts. Therefore, the developed systems are

promising materials for potential use as injectable scaffolds in tissue engineering. On the other hand, because the hydrogels containing the medium (0.055 $mg_{CNTs}/mL_{chit.salt}$) and the highest (0.1 $mg_{CNTs}/mL_{chit.salt}$) concentrations of carbon nanotubes exhibited slight and moderate levels of cytotoxicity, it would be advisable to conduct, in the future, studies in a cancer cell model. If the nanocomposite hydrogels induced higher levels of cytotoxicity towards cancer cells than those observed with a normal human cell line, then targeted cancer therapy could be a potential application for these chitosan systems.

5. Funding

This research was funded by the Young Scientists Fund at the Faculty of Process and Environmental Engineering at the Lodz University of Technology, Poland [grant number: 501/10-34-2-7058], and the funds of the Medical University of Lodz.

6. Author Contributions

Conceptualisation, K.P.; methodology, K.P., Z.M., I.M., and G.G.; formal analysis, K.P. and G.G.; investigation, K.P. and G.G.; resources, K.P., Z.M., and I.M.; writing—original draft preparation, K.P.; writing—review and editing, Z.M. and K.P.; visualisation, K.P. and G.G.; supervision, K.P. and Z.M.; project administration, K.P.; funding acquisition, K.P. and I.M. All authors have read and agreed to the published version of the manuscript.

7. References

[1] Stodolak E, Frączek-Szczypta A, Błażewicz M; (2010) Nanokompozyty polimerowe do zastosowań medycznych. Kompozyty 10(4), 322–327.

[2] Thadathil N, Velappan SP; (2014) Recent developments in chitosanase research and its biotechnological applications: a review. Food Chemistry 150, 392–399. **DOI:** 10.1016/j.foodchem.2013.10.083

[3] Chen Q, Qi Y, Jiang Y, Quan W, Luo H, Wu K, Li S, Ouyang Q; (2022) Progress in research of chitosan chemical modification technologies and their applications. Marine Drugs 20(8), 536. **DOI:** 10.3390/md20080536

[4] Dambuza A, Mokolokolo PP, Makhatha ME, Sibeko MA; (2025) Pharmacological and biological efficacy of chitosan-based materials. International Journal of Molecular Sciences 26(21), 10735. **DOI:** 10.3390/ijms262110735

[5] Edo GI, Yousif E, Al-Mashhadani MH; (2024) Chitosan: an overview of biological activities, derivatives, properties, and current advancements in biomedical applications. Carbohydrate Research 542, 109199. **DOI:** 10.1016/j.carres. 2024.109199

[6] Pieklarz K, Modrzejewska Z; (2021) SARS-COV-2 – The latest global threat and the prospect of COVID-19 therapy with the use of chitosan. Progress on Chemistry and Application of Chitin and its Derivatives 26, 41–60. **DOI:** 10.15259/ PCACD.26.004

[7] El-hefian EA, Nasef MM, Yahaya AH; (2011) Chitosan physical forms: a short review. Australian Journal of Basic and Applied Sciences 5(5), 670–677.

[8] Fatullayeva S, Tagiyev D, Zeynalov N, Mammadova S, Aliyeva E; (2022) Recent advances of chitosan-based polymers in biomedical applications and

environmental protection. Journal of Polymer Research 29(7), 259. **DOI:** 10.1007/s10965-022-03121-3

[9] Bordes P, Pollet E, Avérous L; (2009) Nano-biocomposites: biodegradable polyester/nanoclay systems. Progress in Polymer Science 34(2), 125–155. **DOI:** 10.1016/j.progpolymsci.2008.10.002

[10] Pieklarz K, Tylman M, Modrzejewska Z; (2020) Current progress in biomedical applications of chitosan-carbon nanotube nanocomposites: a review. Mini-Reviews in Medicinal Chemistry 20(16), 1619–1632. **DOI:** 10.2174/1389557520666200513120407

[11] Hernández-Vargas J, González-Campos JB, Lara-Romero J, Prokhorov E, Luna-Bárcenas G, Aviña-Verduzco JA, González-Hernández JC; (2014) Chitosan/MWCNTs-decorated with silver nanoparticle composites: dielectric and antibacterial characterization. Journal of Applied Polymer Science 131(9), 40214. **DOI:** 10.1002/app.40214

[12] Venkatesan J, Jayakumar R, Mohandas A, Bhatnagar I, Kim SK; (2014) Antimicrobial activity of chitosan-carbon nanotube hydrogels. Materials 7(5), 3946–3955. **DOI:** 10.3390/ma7053946

[13] El-Tohamy N, Attia M, Easa SM, Awad NM; (2018) Characterization and evaluation of nanocomposites chitosan-multiwalled carbon nanotubes as broad-spectrum antibacterial agent. Journal of Scientific Research in Science 35, 16–27. **DOI:** 10.21608/JSRS.2018.26727

[14] Qi X, Rui Y, Fan Y, Chen H, Ma N, Wu Z; (2015) Galactosylated chitosan-grafted multiwall carbon nanotubes for pH-dependent sustained release and hepatic tumor-targeted delivery of doxorubicin in vivo. Colloids and Surfaces B: Biointerfaces 133, 314–322. **DOI:** 10.1016/j.colsurfb.2015.06.003

[15] Karnati KR, Wang Y; (2018) Understanding the co-loading and releasing of doxorubicin and paclitaxel using chitosan functionalized single-walled carbon nanotubes by molecular dynamics simulations. Physical Chemistry Chemical Physics 20(14), 9389–9400. **DOI:** 10.1039/C8CP00124C

[16] Abad FRA, Pourmadadi M, Abdouss M, Behzadmehr R, Rahdar A, Pandey S; (2023) Chitosan-carbon nanotube composite: an approach for controlled release of quercetin, modified with carboxymethyl cellulose, for potential anti-cancer therapy. Inorganic Chemistry Communications 158 (Part 2), 111621. **DOI:** 10.1016/j.inoche.2023.111621

[17] Kumar A, Jena PK, Behera S, Lockey RF, Mohapatra S; (2005) Efficient DNA and peptide delivery by functionalized chitosan coated single-wall carbon nanotubes. Journal of Biomedical Nanotechnology 1(4), 392–396. **DOI:** 10.1166/jbn.2005.052

[18] Liu Y, Yu ZL, Zhang YM, Guo DS, Liu YP; (2008) Supramolecular architectures of β-cyclodextrin-modified chitosan and pyrene derivatives mediated by carbon nanotubes and their DNA condensation. Journal of the American Chemical Society 130(31), 10431–10439. **DOI:** 10.1021/ja802465g

[19] Liu X, Zhang Y, Ma D, Tang H, Tan L, Xie Q, Yao S; (2013) Biocompatible multi-walled carbon nanotube-chitosan-folic acid nanoparticle hybrids as GFP gene delivery materials. Colloids and Surfaces B: Biointerfaces 111, 224–231. **DOI:** 10.1016/j.colsurfb.2013.06.010

[20] Cunha MR *et al.*; (2017) In vivo study of the osteoregenerative potential of polymer membranes consisting of chitosan and carbon nanotubes. Materials Research 20(3), 819–825. **DOI:** 10.1590/1980-5373-mr-2016-1112

[21] Zhao W, Yu W, Zheng J, Wang Y, Zhang Z, Zhang D; (2014) Effects of carbon nanotubes in a chitosan/collagen-based composite on mouse fibroblast cell proliferation. Cellular and Molecular Neurobiology 34(1), 43–50. **DOI:** 10.1007/s10571-013-9985-9

[22] Mirmusavi MH, Ahmadian M, Karbasi S; (2022) Polycaprolactone-chitosan/multi-walled carbon nanotube: A highly strengthened electrospun nanocomposite scaffold for cartilage tissue engineering. International Journal of Biological Macromolecules 209 (Part B), 1801–1814. **DOI:** 10.1016/j.ijbiomac.2022.04.152

[23] Sang S, Cheng R, Cao Y, Yan Y, Shen Z, Zhao Y, Han Y; (2022) Biocompatible chitosan/polyethylene glycol/multi-walled carbon nanotube composite scaffolds for neural tissue engineering. Journal of Zhejiang University-SCIENCE B 23(1), 58–73. **DOI:** 10.1631/jzus.B2100155

[24] Mani V, Govindasamy M, Chen SM, Chen TW, Kumar AS, Huang ST; (2017) Core-shell heterostructured multiwalled carbon nanotubes@reduced graphene oxide nanoribbons/chitosan, a robust nanobiocomposite for enzymatic biosensing of hydrogen peroxide and nitrite. Scientific Reports 7(1), 11910. **DOI:** 10.1038/s41598-017-12050-x

[25] Samadi Pakchin P, Ghanbari H, Saber R, Omidi Y; (2018) Electrochemical immunosensor based on chitosan-gold nanoparticle/carbon nanotube as a platform and lactate oxidase as a label for detection of CA125 oncomarker. Biosensors and Bioelectronics 122, 68–74. **DOI:** 10.1016/j.bios.2018.09.016

[26] Carrero-Sánchez JC, Elías AL, Mancilla R, Arrellín G, Terrones H, Laclette JP, Terrones M; (2006) Biocompatibility and toxicological studies of carbon nanotubes doped with nitrogen. Nano Letters 6(8), 1609–1616. **DOI:** 10.1021/nl060548p

[27] Harrison BS, Atala A; (2007) Carbon nanotube applications for tissue engineering. Biomaterials 28(2), 344–353. **DOI:** 10.1016/j.biomaterials.2006.07.044

[28] Błażewicz S, Marciniak J (eds); (2016) Inżynieria biomedyczna: podstawy i zastosowania. T.4, Biomateriały. Akademicka Oficyna Wydawnicza EXIT, Warszawa.

[29] Mantha S, Pillai S, Khayambashi P, Upadhyay A, Zhang Y, Tao O, Pham HM, Tran SD; (2019) Smart hydrogels in tissue engineering and regenerative medicine. Materials 12(20), 3323. **DOI:** 10.3390/ma12203323

[30] Fan R, Cheng Y, Wang R, Zhang T, Zhang H, Li J, Song S, Zheng A; (2022) Thermosensitive hydrogels and advances in their application in disease therapy. Polymers 14(12), 2379. **DOI:** 10.3390/polym14122379

[31] Lv T, Chen Y, Li N, Liao X, Heng Y, Guo Y, Hu K; (2025) A comprehensive review of thermosensitive hydrogels: mechanism, optimization strategies, and applications. Gels 11(7), 544. **DOI:** 10.3390/gels11070544

[32] Yu J, Grossiord N, Koning CE, Loos J; (2007) Controlling the dispersion of multi-wall carbon nanotubes in aqueous surfactant solution. Carbon 45(3), 618–623. **DOI:** 10.1016/j.carbon.2006.10.010

[33] Liu H, Nishide D, Tanaka T, Kataura H; (2011) Large-scale single-chirality separation of single-wall carbon nanotubes by simple gel chromatography. Nature Communications 2(1), 309. **DOI:** 10.1038/ncomms1313

[34] Shi Y, Ren L, Li D, Gao H, Yang B; (2013) Optimization conditions for single-walled carbon nanotubes dispersion. Journal of Surface Engineered Materials and Advanced Technology 3(1), 6–12. **DOI:** 10.4236/jsemat.2013.31002

[35] Pieklarz K, Modrzejewska Z; (2025) Formation mechanism of thermosensitive chitosan hydrogels containing uridine 5'-monophosphate disodium salt. Progress

on Chemistry and Application of Chitin and its Derivatives 30, 254–265. **DOI:** 10.15259/PCACD.30.018

[36] Pieklarz K, Galita G, Majsterek I, Owczarz P, Modrzejewska Z; (2024) Nanoarchitectonics and biological properties of nanocomposite thermosensitive chitosan hydrogels obtained with the use of uridine 5'-monophosphate disodium salt. International Journal of Molecular Sciences 25(11), 5989. **DOI:** 10.3390/ijms25115989

[37] Pieklarz K, Galita G, Tylman M, Maniukiewicz W, Kucharska E, Majsterek I, Modrzejewska Z; (2021) Physico-chemical properties and biocompatibility of thermosensitive chitosan lactate and chitosan chloride hydrogels developed for tissue engineering application. Journal of Functional Biomaterials 12(2), 37. **DOI:** 10.3390/jfb12020037

[38] Nawaz MAH, Rauf S, Catanante G, Nawaz MH, Nunes G, Marty JL, Hayat A; (2016) One step assembly of thin films of carbon nanotubes on screen printed interface for electrochemical aptasensing of breast cancer biomarker. Sensors 16(10), 1651. **DOI:** 10.3390/s16101651

[39] Nascimento RIDC, Vasconcellos R, Fayer de Almeida Campos LB, de Oliveira ER, Ferreira CDSA, Ladeira LO, de Oliveira LFC, Maranduba CMDC, Munk M; (2026) Chitosan films incorporating cellulose nanofibers or carbon nanotubes differentially modulate early responses of stem cells from human exfoliated deciduous teeth. ACS Applied Bio Materials 9(8), 3923–3933. **DOI:** 10.1021/acsabm.6c00220

[40] Wiśniewska-Wrona M, El Fray M; (2019) Physicochemical and functional properties of polymer biocomposites. Polimery 64(1), 23–33. **DOI:** 10.14314/polimery.2019.1.3

[41] Sakurai K, Maegawa T, Takahashi T; (2000) Glass transition temperature of chitosan and miscibility of chitosan/poly(N-vinyl pyrrolidone) blends. Polymer 41(19), 7051–7056. **DOI:** 10.1016/S0032-3861(00)00067-7

[42] Zeng W, Huang J, Hu X, Xiao W, Rong M, Yuan Z, Luo Z; (2011) Ionically cross-linked chitosan microspheres for controlled release of bioactive nerve growth factor. International Journal of Pharmaceutics 421(2), 283–290. **DOI:** 10.1016/j.ijpharm.2011.10.005

[43] Foudazi R, Zowada R, Manas-Zloczower I, Feke DL; (2023) Porous hydrogels: present challenges and future opportunities. Langmuir 39(6), 2092–2111. **DOI:** 10.1021/acs.langmuir.2c02253

[44] Anwesha N, Sagadevan S, Moharana S; (2024) Carbon Nanotube-Polymer Nanocomposites: Spectroscopic, Physiochemical, Electrochemical, and Recent Applications. In: Moharana S, Rout L, Sagadevan S (eds.), Carbon Nanotube-Polymer Nanocomposites, Springer Nature Singapore, Singapore, pp. 105–131. **DOI:** 10.1007/978-981-97-6329-0_5

[45] Chajra H, Auriol D, Joly F, Pagnon A, Rodrigues M, Allart S, Redziniak G, Lefevre F; (2016) Reactivating the extracellular matrix synthesis of sulfated glycosaminoglycans and proteoglycans to improve the human skin aspect and its mechanical properties. Clinical, Cosmetic and Investigational Dermatology 9, 461–472. **DOI:** 10.2147/CCID.S116548

[46] Biological evaluation of medical devices - Part 5: Tests for in vitro cytotoxicity. ISO 10993-5:2009; (2009). International Organization for Standardization, Switzerland.

[47] Dahl JE, Frangou-Polyzois MJ, Polyzois GL; (2006) In vitro biocompatibility of denture relining materials. Gerodontology 23(1), 17–22. **DOI:** 10.1111/j.1741-2358.2006.00103.x

© Polish Chitin Society
Open Access: This article is distributed under the terms of the Creative Commons Attribution 4.0 International License (CC BY 4.0), which permits use, sharing, adaptation, distribution and reproduction in any medium or format, provided that appropriate credit is given to the original author(s) and source, a link to the license is provided, and any changes are indicated. Third-party material is included under the same license unless otherwise stated in a credit line.